Proceedings, 18th International Conference on Offshore Mechanics and Arctic Engineering July 11-16, 1999, St. Johns, Newfoundland

OMAE99-4068

CHARACTERISTICS OF THE WAVE RESPONSE OF MOBILE OFFSHORE BASES

H.R. Riggs
Department of Civil Engineering
University of Hawaii
Honolulu, Hawaii, 96822, USA

R.C. Ertekin
Department of Ocean Engineering
University of Hawaii
Honolulu, Hawaii, 96822, USA

ABSTRACT

Proposals for mobile offshore bases include linking serially 3 to 5 large semisubmersibles to form a platform long enough to support large aircraft. We investigate herein the linear, wave-induced response characteristics of serially-connected semisubmersibles, with the forces required to link the modules as the primary focus. The impact of two connection strategies and structural damping on the response is investigated, and the response 'modes' which contribute to the connector forces are evaluated in detail. We show that the response characteristics can be impacted significantly by the connection strategy. The wet natural frequencies and normal modes are determined and used to explain the response characteristics. Although the analyses are based on a specific semisubmersible design, the results provide insight on how similar systems of connected semisubmersibles may behave.

Key Words: Mobile Offshore Base, Connector Loads, Fluid-structure Interaction, Hydroelasticity

INTRODUCTION

A floating mobile offshore base (MOB) (see, e.g., Remmers et al., 1998) would quite possibly involve connecting several, more traditional-sized semisubmersibles. A MOB could provide logistical support, such as the stationing of several thousand personnel and stockpiling supplies and materiel, in locales where other facilities are not available. To support air operations, a MOB would have to be at least 1500 m long. Operations in deep, unprotected waters and mobility requirements favor connecting three to five semisubmersibles, each 300 to 500 m long. One option is to use mechanical connectors. Such connectors would be subject to large forces. Because semisubmersible design, analysis, and construction technologies have been well-developed and proven in the oil industry, the principle technological questions for this class of MOB relate to the connection.

The objective of this paper is to evaluate the response characteristics of this class of MOB. Our primary goal is to develop a fundamental understanding of how such a structure responds, how the connection strategy can affect that response, and what response modes contribute materially to the connector forces.

To evaluate the linear, wave-induced behavior of serially-connected semisubmersibles, we analyze a 5-module, 1500 m MOB using linear hydroelasticity (see, e.g., Wu, 1984) and the rigid module-flexible connector (RMFC) model (Wang et al., 1991). The operational draft is 39 m, and each module is a two-pontoon, eight-column semisubmersible with approximate dimensions of 300 m x 152 m x 72 m. We consider the impact on the response of two connection options (deck connection and deck-pontoon connection) as well as structural damping. We consider 'wet' natural frequencies, transfer functions in regular seas, and extreme response in irregular seas in the evaluation. A major focus is the response modes which contribute to the connector forces. We show that significant cancellation of modal contributions to the forces can occur. The results reveal how systems of serially-connected semisubmersibles would likely behave. A somewhat complementary study has been reported recently for smaller semisubmersibles, involving flexible modules which are integrally connected (Iijima et al., 1998).

MATHEMATICAL MODEL

We used a linear analysis procedure to determine the wave-induced response. We review briefly here the fundamental assumptions and theory; further details can be found elsewhere (Riggs et al., 1998a and 1998b). The structurally-simple rigid module-flexible connector (RMFC) model was used. This model is appropriate for two situations: 1) relatively stiff modules are joined by relatively flexible connectors, such that virtually all deformations occur in the connectors; and 2) the RMFC model is

a lumped-parameter model of connected flexible modules, in which case the model stiffness represents a lumping of both module and physical connector stiffnesses. The connectors were modeled as linear, 'zero-length,' translational springs. The 'zero-length' assumption is acceptable as long as the connector dimensions are small compared to the module dimensions, which is the case herein. In the RMFC model, the MOB's motions are completely characterized by the 6 displacement degrees-of-freedom of each module (i.e., the modules' surge, sway, heave, roll, pitch and yaw). Although the structural model is simplified, three-dimensional, linear potential theory was used to determine the fluid forces.

We assume the MOB is freely floating in deep water with zero forward speed. The hydrodynamic forces result from the structural motion and from a train of regular long-crested waves with frequency ω, a crest at $x_1 = 0$ (at time $t = 0$), and an incidence angle of β (see Fig. 1). The modules are partially submerged in an incompressible and inviscid fluid undergoing irrotational flow in deep water. The fluid and structural motions are assumed small. The applicable boundary-value problem is well-known; see Wu et al. (1993) and Ertekin et al. (1993) for details. The solution to the boundary value problem was obtained by the well-known, constant panel, 3-D source distribution method. Note that complete structure-fluid-structure interaction involving all modules is considered in determining the added mass matrix, $\mathbf{M}_f$, the hydrodynamic damping matrix, $\mathbf{C}_f$, and the vector of wave exciting forces, $\mathbf{F}_w$.

Given the above assumptions, the complex equations of motion in the frequency domain can be written as

$$[-\omega^2(\mathbf{M}_s + \mathbf{M}_f) + i(\omega\mathbf{C}_f + \mathbf{C}_s) + (\mathbf{K}_s + \mathbf{K}_f)]\mathbf{u} = \mathbf{F}_W \qquad (1)$$

in which **M**, **C**, and **K** refer to 6*N*x6*N* mass, damping, and stiffness matrices, respectively; *N* is the number of semisubmersibles; the subscripts *s* and *f* denote structural and fluid-related quantities, respectively; **u** is the 6*N* vector of module displacements; and the term $e^{i\omega t}$ has been eliminated from both sides of the equation. The transfer functions for the module displacements for a given wave angle β can be obtained by solving Eq. 1 for a range of wave frequencies. The transfer functions for the connector forces can be obtained by appropriate force-displacement relationships. For the present study, the response was determined for frequencies between 0.1 and 1.4 rad/sec, with an interval of 0.05 rad/sec. In addition, 0.175 and 0.225 rad/sec were used, for a total of 29 wave frequencies. Nine wave incidence angles (β = 0˚, 15˚, 30˚, 45˚, 60˚, 75˚, 80˚, 85˚, and 90˚) were considered. The computer program HYDRAN (OCI, 1998) was used for the analyses.

The response in irregular, unidirectional seas has been determined based on the transfer functions. We assume the Rayleigh probability distribution for the wave amplitudes, and therefore the significant response amplitude, R_s, is twice the standard deviation of the response. A measure of the amplitude of the short-term extreme response R_e of any quantity is given by

$$R_e = 1.86R_s = 3.72\sqrt{m_0}, \quad m_0 = \int_0^\infty H^2(\omega)S_\eta(\omega)d\omega \qquad (2)$$

in which $H(\omega)$ is the transfer function of the amplitude-response quantity, and $S_\eta(\omega)$ is the input wave spectrum. The two-parameter Bretschneider wave spectrum, involving the significant wave height H_s and peak period T_p, and five irregular sea states were considered for the present study (H_s = 3.25, 5.00, 7.50, 11.50, 15.25 m and T_p = 9.7, 12.4, 15.0, 16.4, 20.0 sec, respectively). The wave spectra are shown in Fig. 2. Only long-crested seas are considered here.

MOB CHARACTERISTICS

The MOB consists of 5 identical modules with a draft of 39 m. The modules are 300 m x 152 m in plan; other principal characteristics are given in Table 1. The module properties in Table 1 are specified in a 'module' coordinate system, $\bar{x}_1 - \bar{x}_2 - \bar{x}_3$, the origin of which is located at the center of gravity (CG) of the module. Axis $\bar{x}_3$ is directed vertically up, axis $\bar{x}_1$ is directed horizontally parallel to the pontoons, and horizontal axis $\bar{x}_2$ is normal to the pontoons. Motions in the $\bar{x}_1$, $\bar{x}_2$, and $\bar{x}_3$ directions correspond to the module's surge, sway, and heave, respectively. Each module is doubly-symmetric, i.e., they are symmetric with respect to the $\bar{x}_1 - \bar{x}_3$ and the $\bar{x}_2 - \bar{x}_3$ planes.

The hydrodynamic panel mesh for (one-quarter of) the doubly-symmetric single module involves 404 constant strength panels, with 80 panels on each column. A convergence study, which involved increasing the panels by a factor of approximately 4, showed that this discretization adequately captured the module motions. For one-quarter of the doubly-symmetric 5-module MOB, 2,020 panels were used, which is equivalent to 8,080 panels on the entire MOB.

A plan view of the MOB is shown in Fig. 1, which also defines the module numbering scheme and the global coordinate system ($x_1 - x_2 - x_3$, which corresponds to module 3's coordinate system). Connectors are used to join adjacent modules. Each individual connector provides finite resistance to relative translational motions but no resistance to relative rotational motions. Two connection strategies are considered herein. The base case, denoted *kdeck*, involves two connectors between adjacent modules, at the deck level only. The connectors are located at $\bar{x}_2$ = ±50 m and $\bar{x}_3$ = 33.13 m. Longitudinally, the connectors are located 300 m on center. The connector numbering scheme is indicated in Fig. 1, in which c_j refers to connector *j*. There are a total of 8 connectors in this strategy. Additional studies involving this case are reported in Riggs et al. (1998a and 1998b). The second case, denoted *k4*, involves four connectors, two at the deck level and two at the pontoon level, connecting each of the pontoons. The deck level connectors are located as in *kdeck*, and the pontoon connectors are at $\bar{x}_2$ = ±50 m and $\bar{x}_3$ = –18.87 m. The connector numbering scheme is such that modules 1 and 2 are joined by connectors 1 and 2 at the deck level and connectors 3 and 4 at the pontoon level. The sequencing continues similar to that shown in Fig. 1.

As stated previously, each connector is modeled by three translational springs. For *kdeck*, the longitudinal, transverse, and

vertical spring stiffnesses were 10^4, 10^6 and 10^3 MN/m, respectively. These values are based on a study in which the lower natural frequencies of the RMFC model were matched with the corresponding frequencies of a finite element model of the MOB (MEH, 1997). For *k4*, each connector had one-half the stiffness as in the other two cases, which maintains the total translational stiffnesses at the same level. For comparison, the hydrostatic stiffness of a single module in heave, roll, and pitch is 34 MN/m, 4.06 x 10^4 MN-m/rad, and 1.24 x 10^5 MN-m/rad, respectively.

Very stiff connectors may cause numerical ill-conditioning of Eq. 1. However, we calculated the residual errors of the solutions, and they were within acceptable tolerances for all frequencies.

'WET' NATURAL FREQUENCIES AND NORMAL MODES

To gain an understanding of the natural vibration characteristics of the connected MOB, we determined 'wet' natural frequencies, ω_n, and normal modes, $\boldsymbol{\psi}_n$, from the undamped, homogeneous form of Eq. 1:

$$[-\omega_n^2(\mathbf{M}_s + \mathbf{M}_f) + (\mathbf{K}_s + \mathbf{K}_f)]\boldsymbol{\psi}_n = \mathbf{0} \tag{3}$$

Because the added mass matrix, $\mathbf{M}_f$, is frequency-dependent, Eq. 3 represents a real, nonlinear eigenvalue problem. We used an iterative procedure for the solution, in which the added mass was calculated for a wave frequency, ω, and then the natural frequencies were calculated. If a resulting natural frequency was sufficiently close to the wave frequency, it was accepted as an actual natural frequency. The error measure used was $|(\omega-\omega_n)/\omega|*100\%$.

We used the same procedure to determine the natural frequencies of a single, rigid module, which were found to be 0.193, 0.128, and 0.159 rad/sec, for rigid body heave, roll, and pitch respectively. For these frequencies the above error measure is 1.5% or less.

It will be useful to distinguish between 'structural' and 'non-structural' normal modes of the MOB. We classify a normal mode as 'structural' if a significant percent of the total potential energy associated with the normal mode comes from the connectors. Otherwise, it can be concluded that the mode consists primarily of rigid body motions of the modules in such a way that there is relatively little deformation in the connectors.

For both connection cases, the first 3 natural frequencies of the MOB, corresponding to rigid body surge, sway, and yaw, are zero. The fourth natural frequency, corresponding essentially to rigid body roll, is approximately 0.128 rad/sec. These modes are, of course, non-structural.

We list the calculated natural frequencies below 1.4 rad/sec, together with a description of the normal modes, in Table 2 and Table 3 for *kdeck* and *k4*, respectively. All frequencies have an error of less than 6%. An evaluation of the percentage of the total potential energy in the connectors revealed that the modes are classified easily as either structural or non-structural.

For case *kdeck*, the modes denoted 'vertical' involve surge, heave, and pitch of the modules. The indicated symmetry/anti-symmetry is with respect to the x_2–x_3 plane. Mode 5 involves alternating pitch of the modules, resulting in a 'sawtooth' configuration. Modes 6 and 7 are similar to mode 5, involving primarily heave and pitch of the modules. Using a beam analogy, mode 8 has the appearance of the 1st vertical bending mode of a free-free beam. Those modes with a natural frequency closer to the single module pitch natural frequency of 0.159 rad/sec have a substantial pitch component, while those modes with a natural frequency closer to the single module heave natural frequency of 0.193 rad/sec have a substantial heave component. Mode 11, the first structural mode, is analogous to the 1st horizontal bending mode of a free-free beam, and mode 12 corresponds to the 1st torsional mode. (Because the 'shear center' and the center of mass are not coincident, mode 11 also involves slight torsion and mode 12 also involves slight horizontal bending.) The 'dry' natural frequencies (i.e., for the structure 'in-air') corresponding to modes 11 and 12 are 1.09 and 1.33 rad/sec, respectively. It is likely that the connector deformations will be significant primarily if modes 11and/or 12 are excited. It is unlikely that higher modes will be significantly excited because of the low energy content of incident waves at frequencies higher than 1.4 rad/sec, although the spatial distribution of the load must also be considered. Aligning the connectors at the same elevation introduces considerable flexibility related to heave and pitch motions of the modules, as revealed by these non-structural vertical modes.

When the natural frequencies and normal modes for *k4* are compared to those for *kdeck*, several differences can be identified immediately. First, by connecting the deck and pontoons, the connection stiffness is sufficient to cause rigid body pitch of the entire MOB (mode 5), as though it is a rigid body. The vertical 'mechanism-type' modes, with essentially zero energy in the connectors, are eliminated. It can be expected that the forces that excite these modes will now have to be resisted by the connectors, especially through longitudinal forces, which resist relative pitch of the modules. Second, the first vertical bending mode now has a natural frequency, 0.422 rad/sec, at which there is significant wave energy. Hence, resonance leading to large longitudinal connector forces can be expected if the spatial distribution of the wave exciting forces also corresponds to first mode vertical bending. Third, the creation of a 'closed cross section,' by locating connectors at both the top and bottom, has increased the frequency of the first torsional mode to over 1.4 rad/sec.

The increase in the natural frequency of the torsional mode is a positive result of adding connectors at the pontoons. However, the shift of the first structural bending mode into the region at which there is substantial wave energy is a substantially negative result. If the longitudinal connector stiffness is increased by a factor of 8 (a significant amount), the frequencies of modes 5 and 6 are not affected, the frequency of the first structural mode, mode 7, is shifted out of the wave energy region to 0.984 rad/sec, and the frequencies of modes 8 and 9 are shifted beyond 1.4 rad/sec.

HYDRODYNAMIC CONSIDERATIONS

The surge, sway, heave, roll, pitch, and yaw motion characteristics of a single, rigid module are of course very important to the response of serially-connected modules. The motion RAOs

and extreme response of the present semisubmersible design have been presented in detail elsewhere (Riggs et al., 1998a; 1998b) and will not be repeated here. A few comments are in order, however. The module is very large; the 300 m length is nearly three times the length of many semisubmersibles used in the oil industry. The large size results in motions which are in general smaller than would otherwise occur. Also, as stated before, the heave, roll and pitch natural frequencies are low, and they are below the frequency range with significant wave energy. Also reported in Riggs et al. (1998a and 1998b) are the results of serially-positioned but unconnected modules. The results illustrate that the structure-fluid-structure interaction of these modules is not large. Those quantities most impacted by the presence of adjacent modules are surge and pitch in head seas.

CONNECTION STRATEGY AND DAMPING

Prior to a detailed investigation of the wave-induced response of a MOB, it is useful to consider first the extreme response for the two cases to determine the impact of connector location and structural (connector) damping. Figs. 3 and 4 present the maximum extreme motions for the MOB modules. The results shown are the maximum response, considering all modules and the seastates and wave angles specified previously. The maxima are shown for three hysteretic structural damping ratios: 0%, 2%, and 5%. Inspection of these figures demonstrates that for *kdeck* the structural damping, at least for ratios up to 5%, does not affect the maximum motions. The response of *k4* demonstrates the response is significantly affected by introducing connectors at the pontoon. Heave is much higher than for the other two cases. In addition, heave and pitch are reduced significantly by structural damping, which implies that resonance of mode 7 is significant.

The maxima of the extreme connector forces, considering all connectors, are shown in Fig. 5. For *kdeck*, connector damping reduces the horizontal connector forces by approximately 15%, which could be significant for design. The horizontal connector forces are substantially larger for *k4*, and damping causes a substantial reduction, neither of which is surprising given the natural frequency of the first vertical bending mode.

Providing 5% structural damping would be difficult to achieve and would require innovative design. It is possible that such a level of additional damping might be achieved not just through connector design, but also through the addition of 'hydrodynamic' components to increase, for example, energy dissipation through viscous damping. The difficulties notwithstanding, in the following discussion 5% damping will be considered, given the beneficial reduction that damping can produce.

CONNECTOR FORCES

Because a major motivation of this study is to understand more completely the forces required to link semisubmersible modules, we examine these forces in detail. Space limitations require us to focus exclusively on longitudinal connector forces. As can be seen from Fig. 5, these are substantially larger than the transverse and vertical forces. Fig. 6 shows the maximum extreme longitudinal connector forces, considering all connectors, as a function of seastate and wave angle. The maximum forces occur in near beam seas, a result which has been discussed previously (Wu and Mills, 1996; Riggs et al., 1998a and1998b). The results for the transverse and vertical connector forces are similar, except that the magnitudes are significantly lower (see Fig. 5).

The connectors associated with module 3 (connectors 3–6) have the highest longitudinal forces, and of these, connector 3 has the largest force. The RAO for this force is shown in Fig. 7. From Fig. 7 it is clear that the reason the highest longitudinal forces occur at 85° is because of the large peak in the RAO at 0.7 rad/sec. It can be shown that first mode longitudinal bending (i.e., mode 11) contributes 93% of the peak value. For an incoming wave at 0.7 rad/sec and 85°, the projected wave length is almost 1500 m; that is, if a crest is at the beginning of the MOB, then a crest is also at the end and a trough is at the middle. Hence, the Froude-Krylov forces are spatially distributed so as to excite first mode horizontal bending. At this excitation frequency, the dynamic magnification factor for mode 11, based on the definition for a single degree-of-freedom system with natural frequency of 0.923 rad/sec, is approximately 2.3.

A decomposition of the RAO into the different response components reveals more clearly how the module relative motions contribute to the force. Relative surge, pitch and yaw contribute to the longitudinal forces. Fig. 8 shows the relative contributions of each of these motions to the RAO for a wave angle of 85°. It is clear that the longitudinal forces are due almost entirely to relative yaw (horizontal bending), and that the forces induced by relative surge and pitch cancel each other. If either surge or pitch were constrained, however, then the connector force could change substantially. Of course, at a wave angle of 0° there is no yaw and the longitudinal force is due solely to relative surge and pitch.

For *k4*, Fig. 9 shows the maximum extreme longitudinal connector forces, considering all connectors, as a function of seastate and wave angle. The maximum forces occur at a wave angle of 75°. Again, connectors associated with module 3 have the highest longitudinal forces (connectors 5, 8, 9, and 12), and of these connector 8 has the largest. The RAO for this force is shown in Fig. 10. A large peak in the RAO occurs at 0.4 rad/sec and 75°. Examination of the incoming wave reveals that the Froude-Krylov forces are distributed such as to excite vertical bending. In addition, the dynamic amplification factor for mode 7 is approximately 7. These results and the significant wave energy near 0.4 rad/sec explains why the longitudinal connector forces are so large for *k4*, and why structural damping is so important. The RAOs for the transverse and vertical connector forces also have peaks at or near 0.4 rad/sec, although the magnitudes are much smaller.

As before, a decomposition of the RAO into the different response components reveals how the module relative motions contribute to the force. Fig. 11 shows that, at low frequencies (0.2–0.5 rad/sec), although the longitudinal force results from a summation of surge, pitch and yaw motions, pitch (vertical bending) is the major contributor, as expected. At larger frequencies (> 0.6 rad/sec), yaw (horizontal bending) is the dominant contrib-

utor.

Because resonance in vertical bending is clearly a problem for *k4*, it is interesting to determine the extreme response when the longitudinal connector stiffness is increased by a factor of 8. As mentioned previously, the frequency of the first vertical bending mode is shifted to 0.984 rad/sec. In this case the extreme longitudinal connector forces are reduced by a factor of approximately 2, as are the vertical forces. The transverse forces are essentially unchanged.

CONCLUSIONS

Based on the current study, the following conclusions can be drawn. It should be noted that they are based on the module design and MOB layout described herein. Although some of these conclusions can be generalized to similar cases, care should be taken in making such generalizations.

1. For the connection strategies and stiffnesses considered here, the longitudinal connector forces are substantially larger than the transverse and vertical connector forces. The extreme longitudinal forces are due to either horizontal bending (*kdeck*) or vertical bending (*k4*). Note that a previous study (Riggs et al., 1998a) found that if the stiffness of *kdeck* is reduced, e.g., by three orders of magnitude, the maximum longitudinal forces result primarily from relative surge. However, the forces for such a soft connection were relatively small.

2. Aligning the connectors at the same elevation to form a 'hinge' connector (*kdeck)* creates a 'non-structural,' mechanism-type vertical bending mode. The natural frequency of this mode is approximately equal to the natural pitch frequency of a single module.

3. Connecting the modules at the deck and pontoons (*k4*) increases substantially the longitudinal connector forces if the natural frequency of the first vertical bending mode is shifted to the frequency range with significant wave energy. Resonance can occur, and structural damping can be important.

4. Structural damping can reduce the calculated extreme longitudinal forces significantly. The reduction caused by 5% damping, relative to no damping, for *kdeck* and *k4* was 15% and 18%, respectively.

5. The wave frequencies and angles corresponding to peaks in the RAOs of the connector forces can be explained, at least partially, by the spatial distribution of the Froude-Krylov forces which excite structural modes involving the specific force.

6. The maximum extreme connector forces occur in wave angles ranging from approximately 75° to approximately 85°. Limiting the wave angle to a maximum of 45° will reduce the maximum longitudinal forces by a factor of approximately 2.

These results are based on the RMFC model. If the flexibility of the modules are explicitly modeled, some differences may result. Such a study is a logical next step in an investigation of response characteristics of connected semisubmersibles. Such a study is currently in progress.

ACKNOWLEDGEMENTS

The authors would like to acknowledge support by the Office of Naval Research, MOB Program, through Float, Inc., San Diego, and by the National Science Foundation under grant BCS-9532037. They would also like to thank McDermott Engineering Houston for the permission to use their MOB design as the basis for the study.

REFERENCES

Ertekin, R. C., Riggs, H. R., Che, X. L. and Du, S. X., 1993, 'Efficient Methods for Hydroelastic Analysis of Very Large Floating Structures, *Journal of Ship Research*, Vol. 37, No. 1, pp. 58-76.

Iijima, K., Suzuki, H. and Yoshida, Y., 1998, 'Structural Response Characteristics of Very Large Semi-Submersible and Design Considerations,' *Proceedings, 17th International Conference on Offshore Mechanics and Arctic Engineering*, Lisbon, OMAE98-4356.

MEH, 1997, 'Mobile Offshore Base (MOB) Preliminary Design Report: Vol. II–Connectors, Motions, and Loads,' Report CDRL Sequence No. C009, McDermott Engineering Houston, LLC, Houston, TX.

OCI, 1998, 'HYDRAN: A Computer Program for the HYDroelastic Response ANalysis of Ocean Structures,' Report v. 1.9.8, OffCoast, Inc., Kailua, HI.

Remmers, G., Zueck, R., Palo, P. and Taylor, R., 1998, 'Mobile Offshore Base', *Proceedings*, *8th International Offshore and Polar Engineering Conference*, Montreal, Vol. 1, pp. 1-5.

Riggs, H. R., Ertekin, R. C. and Mills, T., 1998a, 'Impact of Connector Stiffness on the Response of a Multi-Module Mobile Offshore Base,' *Proceedings*, *8th International Offshore and Polar Engineering Conference*, Montreal, Vol. 1, pp. 200-207.

Riggs, H. R., Ertekin, R. C. and Mills, T., 1998b, 'Wave-Induced Response of a 5-Module Mobile Offshore Base,' *Proceedings, 17th International Conference on Offshore Mechanics and Arctic Engineering*, Lisbon, OMAE98-4440.

Wang, D. Y., Riggs, H. R. and Ertekin, R. C., 1991, 'Three-Dimensional Hydroelastic Response of a Very Large Floating Structure,' *International Journal of Offshore and Polar Engineering*, Vol. 1, No. 4, pp. 307-316.

Wu, C. and Mills, T. R. J., 1996, 'Wave Induced Connector Loads and Connector Design Considerations for the Mobile Offshore Base,' *Proceedings, International Workshop on Very Large Floating Structures*, Hayama, Japan, pp. 387-392.

Wu, Y., 1984, 'Hydroelasticity of Floating Bodies,' Ph.D. dissertation, Brunel University.

Wu, Y. S., Wang, D. Y., Riggs, H. R. and Ertekin, R. C., 1993, 'Composite Singularity Distribution Method with Application to Hydroelasticity,' *Marine Structures*, Vol. 6, No. 2&3, pp. 143-163.

Table 1 Principal characteristics of a module

Upper Hull	
Length	280 m
Breadth	152 m
Depth	24.6 m
Lower Hull	
Length	260 m
Breadth	38 m
Depth	16 m
Transverse Spacing	100 m
Columns	
Length	21 m
Breadth	21 m
Longitudinal Spacing	63 m
Transverse Spacing	100 m
Operational Displacement	337,000 x 10^3 kg
$\bar{I}_1$	1.0493 x 10^{12} kg-m^2
$\bar{I}_2$	2.9273 x 10^{12} kg-m^2
$\bar{I}_3$	3.1744 x 10^{12} kg-m^2
KG	26.87 m

Table 2 Natural frequencies and modes-*kdeck*

	kdeck	
Mode	Frequency (rad/sec)	Description
5	0.153	Non-structural; vertical, antisymmetric
6	0.165	Non-structural; vertical, symmetric
7	0.181	Non-structural; vertical, antisymmetric
8	0.188	Non-structural; 1st vertical bending mode
9	0.192	Non-structural; vertical, antisymmetric
10	0.192	Non-structural; rigid body heave of MOB
11	0.923	Structural; 1st horizontal bending mode
12	0.943	Structural; 1st torsional mode

Table 3 Natural frequencies and modes-*k4*

	k4	
Mode	Frequency (rad/sec)	Description
5	0.192	Non-structural; rigid body pitch of MOB
6	0.192	Non-structural; rigid body heave of MOB
7	0.422	Structural; 1st vertical bending mode
8	0.925	Structural; 1st horizontal bending mode
9	1.05	Structural; 2nd vertical bending mode

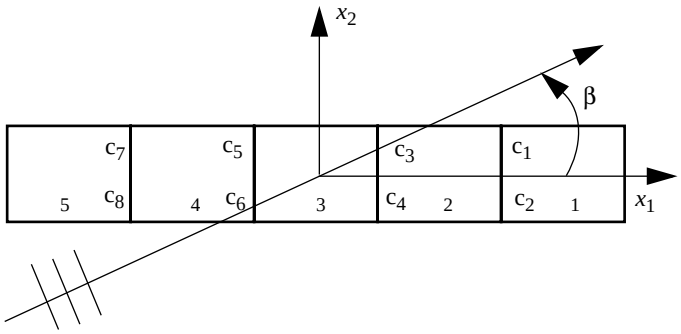

Fig. 1 Definitions of global coordinates, wave angle β, module numbers, and connector numbers

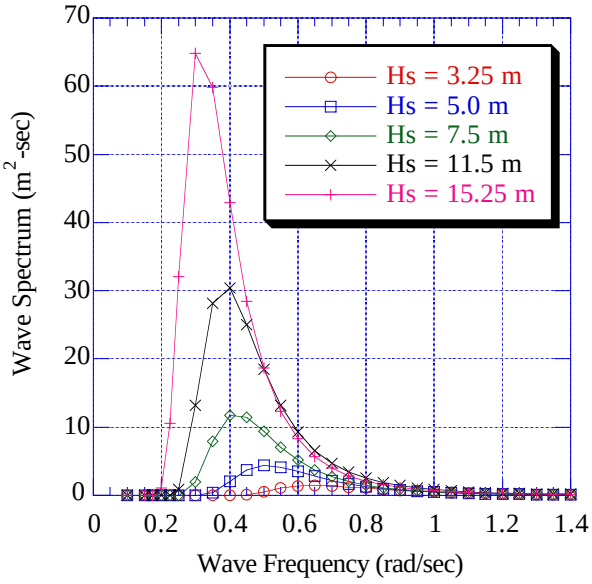

Fig. 2 Bretschneider wave spectra for five significant wave heights

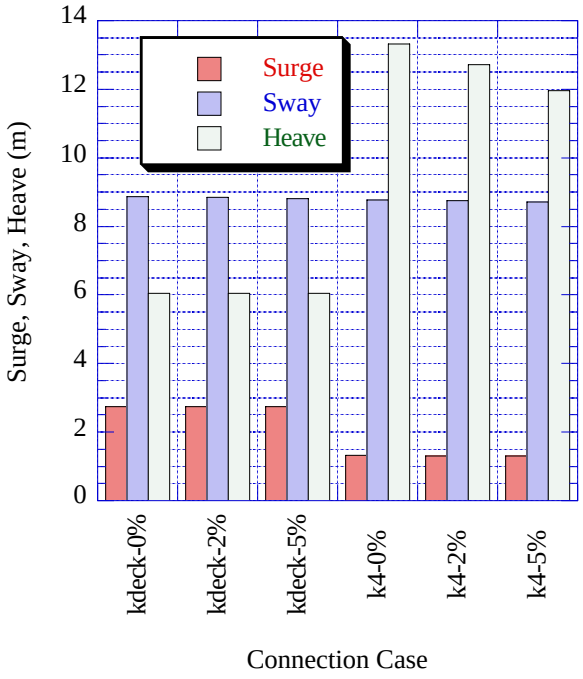

Fig. 3 Maximum extreme surge, sway, and heave for all modules, wave angles, and seastates

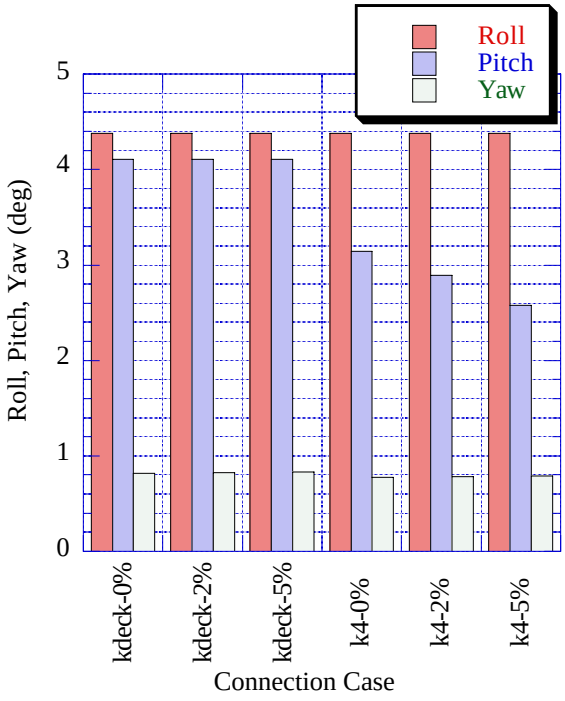

Fig. 4 Maximum extreme roll, pitch, and yaw for all modules, wave angles, and seastates

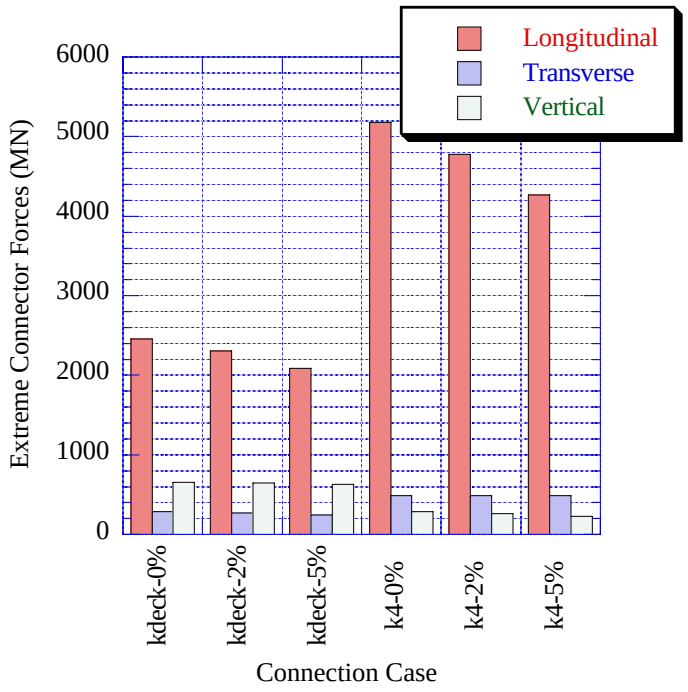

Fig. 5 Maximum extreme connector forces for all connectors, wave angles, and seastates

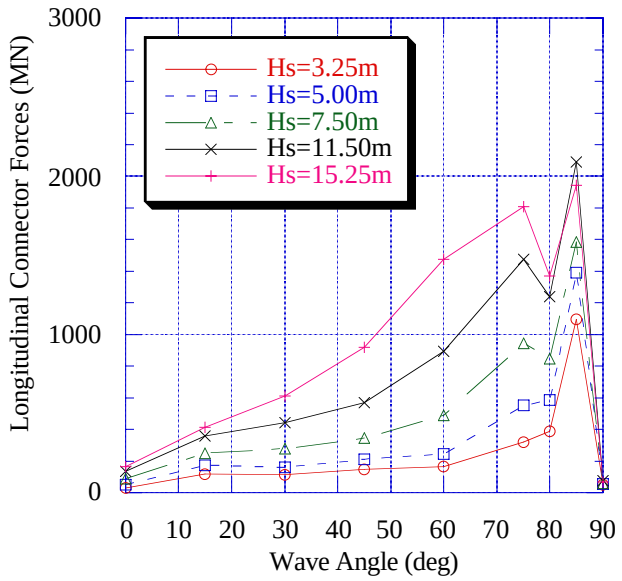

Fig. 6 Extreme longitudinal connector forces–*kdeck*

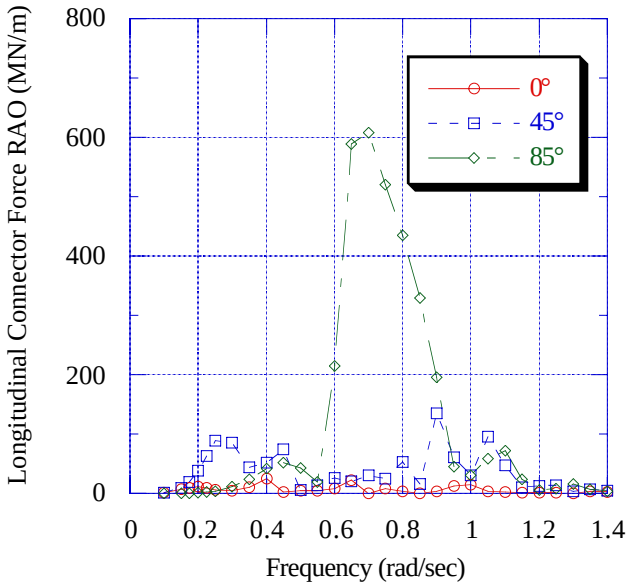

Fig. 7 RAO of longitudinal force in connector 3–*kdeck*

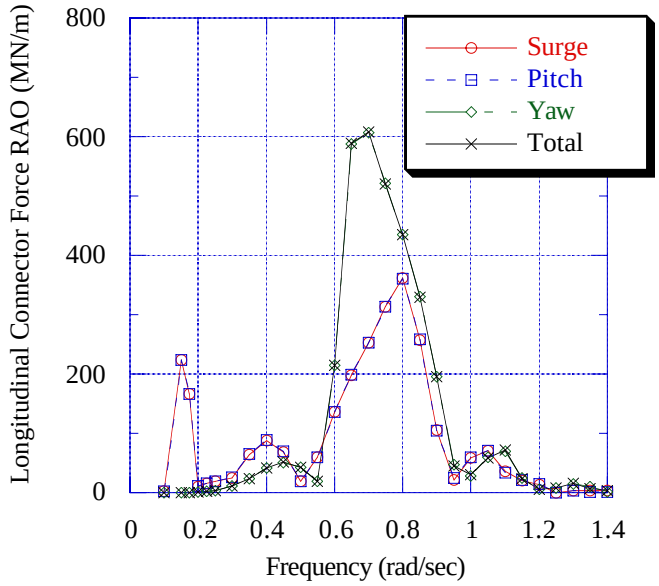

Fig. 8 Composition of RAO of longitudinal force in connector 3 at 85°–*kdeck*

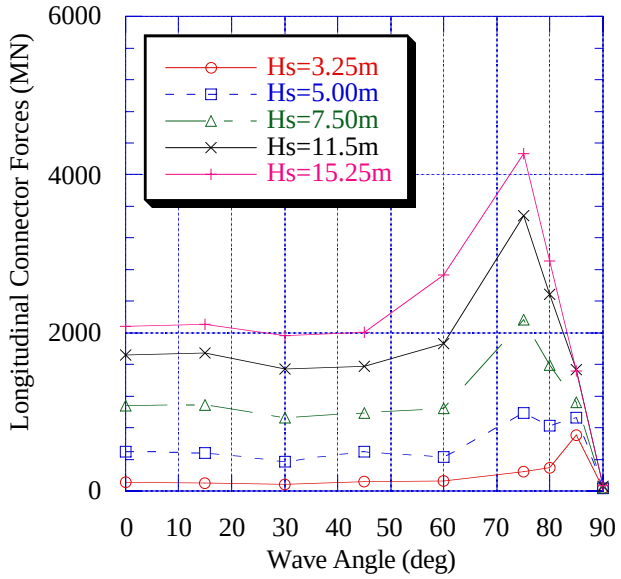

Fig. 9 Extreme longitudinal connector forces–*k4*

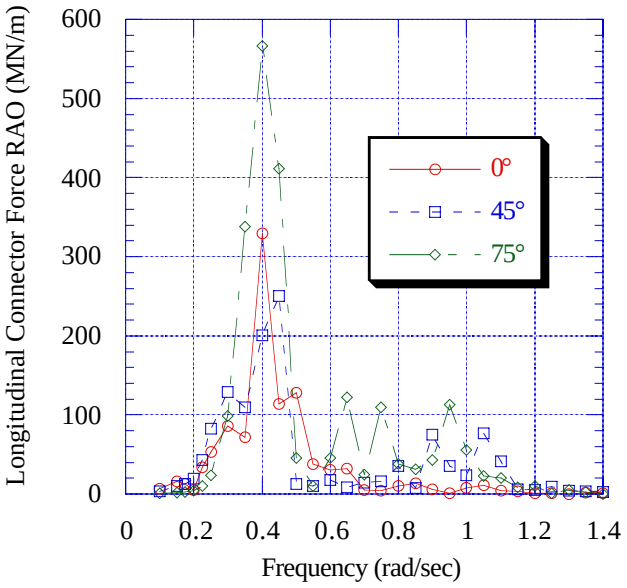

Fig. 10 RAO of longitudinal force in connector 8–*k4*

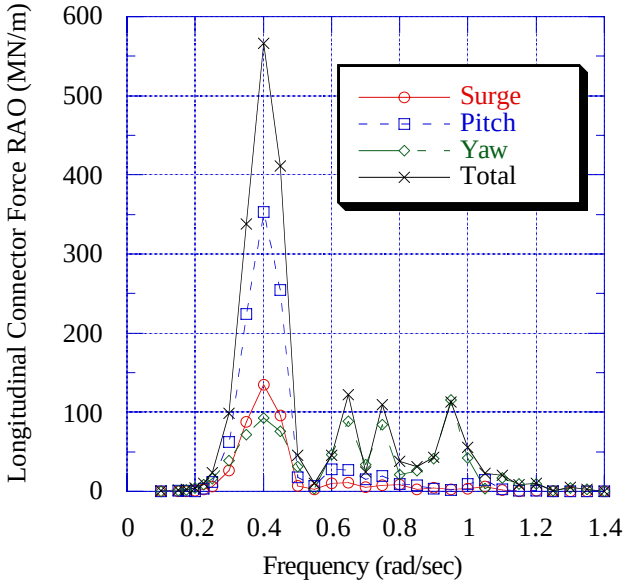

Fig. 11 Composition of RAO of longitudinal force in connector 8 at 75°–*k4*